



Published in final edited form as:

Anal Chem. 2021 March 30; 93(12): 5317–5326. doi:10.1021/acs.analchem.1c00533.

Chemical reactivities of two widely used ruthenium-based CO releasing molecules (CO-RMs) with a range of biologically important reagents and molecules

Zhengan Yuan[#], Xiaoxiao Yang[#], Yuqian Ye, Ravi Tripathi, Binghe Wang^{*}

Department of Chemistry and Center for Diagnostics and Therapeutics, Georgia State University, Atlanta, Georgia 30303, USA;

[#] These authors contributed equally to this work.

Abstract

Ruthenium-based CO releasing molecules (CO-RMs), CORM-2 and CORM-3, have been widely used as surrogates of CO for studying its biological effects *in vitro* and *in vivo* with much success. However, several previous solution-phase and *in-vitro* studies have revealed the ability for such CO-RMs to chemically modify proteins and reduce aromatic nitro groups due to their intrinsic chemical reactivity under certain conditions. In our own work of studying the cytoprotective effects of CO donors, we were in need of assessing chemical factors that could impact the interpretation of results from CO donors including CORM-2,3 in various *in-vitro* assays. For this, we examined the effects of CORM-2,3 toward representative reagents commonly used in various bioassays including resazurin, tetrazolium salts, nitrites and azide-based H₂S probes. We have also examined the effect of CORM-2,3 on glutathione disulfide (GSSG), which is a very important redox regulator. Our studies show the ability for these CO-RMs to induce a number of chemical and/or spectroscopic changes for several commonly used biological reagents under near physiological conditions. These reactions/spectroscopic changes cannot be duplicated with CO-deleted CO-RMs (iCORMs), which are often used as negative controls. Further, both CORM-2 and -3 are capable of consuming and reducing GSSG in solution. We hope the results described will help future design of control experiments in using Ru-based CO-RMs in similar experiments.

Graphical Abstract

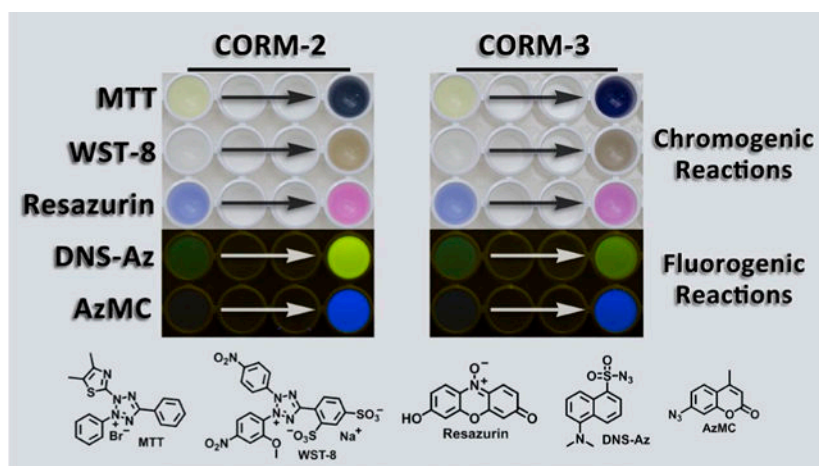
^{*} **Corresponding Author:** wang@gsu.edu.

Supporting Information

The Supporting Information is available free of charge on the ACS Publications website. Additional information and spectroscopic data as noted in text.

Notes

Any additional relevant notes should be placed here.



Ruthenium-based CO releasing molecules, CORM-2 and CORM-3, have intrinsic chemical reactivities toward widely used bioassay reagents such as MTT, WST-8, resazurin and azide-based H_2S probes as well as glutathione.

As an endogenously produced gaseous molecule, carbon monoxide (CO) has been well demonstrated by many studies to possess signaling roles in mammals.¹ More importantly, the therapeutic effects of CO have been validated extensively in various disease models, including colitis, inflammatory sepsis, drug-induced organ toxicity and others.^{2–6} Earlier studies employed inhalation form of CO.^{2, 7} However, limitations such as the need for a special inhalation device, risk to patients and healthcare workers, and difficulties in controlling dosage^{2, 8} led many to search for delivery forms that are more compatible for wide-spread use.^{2, 4, 9–11} Along this line, Motterlini and Mann pioneered the use of metal-immobilized carbonyls as CO-releasing molecules (CO-RMs)^{2, 12–15} with much success; many others also reported very interesting CO-RMs.^{16–19} Among all the metal-based CORMs, two ruthenium-based, CORM-2 and CORM-3, are probably the most widely used as CO donors in a large number of studies. A quick PubMed search of “CORM-2 OR CORM-3” led to about 500 hits, demonstrating the broad impact of these two CO-RMs. Later efforts in developing CO donors led to photo-sensitive organic CO-RMs^{20–26} and organic CO prodrugs (Figure 1).^{27–30}

As shown in Figure 1, CORM-2 and CORM-3 are both ruthenium-carbonyl complexes and have been reported to transfer CO spontaneously under physiological conditions.^{2, 14, 15} In a typical study using a metal-based CO-RM, the depleted CO-RM after CO release (iCO-RM) is used as the negative control. The inactive form of CORM-2 (iCORM-2) is commonly prepared by incubation of CORM-2 with DMSO for 18 h, which leads to ligand-exchange reactions to liberate CO, yielding a mixture of decomposition products.^{15, 31} The final dicarbonyl products (Complex B and C) have been reported to be incapable of releasing CO (Figure 2).³¹ Inactive CORM-3 (iCORM-3) is normally prepared by incubation of CORM-3 in buffer (Krebs-Henseleit or PBS, pH 7.4) for 18 h, and the resulting solutions have been reported to show no CO release as measured using the myoglobin assay.¹² Therefore, such solutions have been widely used as iCORM-3 stock solutions for providing a negative

control in CORM-3 related studies. However, the composition and structure of iCORM-3 products have not been well characterized.

An ideal CO donor, whether a metal-based CO-RM or an organic CO prodrug, should have minimal CO-independent effects. If it does, then the negative control should duplicate such CO-independent effects in order to assess the true effect of CO. Sporadic studies indicated that some of the reported biological effects of metal-based CORMs such as CORM-2 and CORM-3 cannot be attributed to their ability to donate CO.^{19, 32–45} These observed biological effects were said to be CO-independent by the respective authors. Additional studies reported some unique chemical reactivities of ruthenium-based CO-RMs in solution.^{31, 46–48} For example, Poole and coworkers used NMR to determine the K_d between CORM-3 and biological thiol species (cysteine and glutathione) to be about 5 μM .³² Heinemann and coworkers reported the CO-independent functions on K^+ channels by CORM-2.⁴³ Nielsen described that the widely studied effect of CORM-2 against snake venom was through a CO-independent mechanism.³⁴ Stahl and colleagues described the intrinsic ability for CORM-2 to consume molecular oxygen in solution.³⁷ In aqueous medium ($\text{pH} > 3$), early solution studies found that $[\text{Ru}(\text{CO})_3]^{2+}$ can react with OH^- to form metallacarboxylate species, which undergoes further decomposition to generate potential reducing agents such as Ru-hydrides and Ru(0) carbonyl complexes.^{31, 49–51} Zero-valent ruthenium carbonyl complex, $\text{Ru}_3(\text{CO})_{12}$, has been used as a reducing agent for aromatic nitro compounds (Figure S1).^{50, 51} Along a similar line, we have also reported that that CORM-3 is capable of reducing an aryl nitro group to an amino group under near-physiological conditions, and such effects cannot be achieved by iCORM or CO from other sources including CO gas.⁴¹ In our own work of studying the cytoprotective effects of CO donors, we were in need of assessing biochemical factors that could impact the interpretation of cell culture results from CO donors including CORM-2,3. All these led us to systemically probe the chemical reactivity of these two ruthenium-based CO-RMs with reagents commonly used in cellular assays such as resazurin, tetrazolium salts, nitrite and azide-based H_2S probes with the hope of deconvoluting factors that need to be carefully considered and controlled in designing future experiments. Further, sulfide and the thiol group are known to be very important in cellular redox regulation and as antioxidants. We also probed the effect of CORM-2,3 on glutathione disulfide (GSSG) as a representative bio-disulfide because of its known roles in cellular signaling and redox regulations.^{52, 53} It was found that both CORM-2 and CORM-3 have intrinsic reactivities toward these bioassay reagents and are capable of consuming and reducing GSSG. However, it should be noted that these chemical reactivities should only be interpreted in the context of the experimental conditions and should not be extrapolated to animal models and cell culture conditions. How such findings would affect the interpretations of results from each specific biological study is beyond the scope of this study, and is best left to experts who are most familiar with the interpretation of the biological problems examined in each study. This study primarily focuses on the chemical reactivity and molecular events when incubating with a commonly used reagent. We hope that our results will help future design of biological experiments using CORM-2,3 and associated controls.

EXPERIMENTAL SECTION

General information.

All reagents and solvents were of reagent grade from commercial suppliers (Sigma Aldrich and etc.). ^1H (400 MHz) NMR spectra were acquired on a Bruker-400 spectrometer. Fluorescence spectra were recorded on a Shimadzu RF-5301PC fluorometer. Absorption spectra were measured on Varian Cary 100 Bio UV-Visible spectrophotometer. A microplate reader (PerkinElmer Victor2, USA) was used for resazurin and CCK-8 assay. LC-MS data were collected on a Shimadzu LCMS-2010 system. GC-TCD studies were performed on an Agilent 7820A system. CO-RMs (CORM-2, CORM-3, CORM-A1 and CORM-401) and H_2S probe (AzMC) were purchased from Sigma-Aldrich and were used without purification. Pure CO gas was purchased from Airgas company. iCORM-2 and iCORM-3 were prepared according to the literature procedures.^{12, 54} CO prodrugs (CO-103 and CO-111)^{27, 55} and H_2S probe (DNS-Az)⁵⁶ were synthesized according to the literature procedures.

Preparation of stock solutions.

Stock solutions of CORM-2 (10 mM), CORM-401 (10 mM), CO-103 (10 mM), CO-111 (10 mM), resazurin (1 mM) and AzMC (1 mM) were prepared in DMSO. 10 mM Stock solutions of CORM-3, CORM-A1, MTT and WST-8 were prepared in water. 100 mM stock solution of monobromobimane (mBBr) was prepared in acetonitrile. MTT formazan was dissolved in isopropanol to afford a 2 mM stock solution. DNS-Az was dissolved in ethanol to afford a 30 mM stock solution. 200 \times stock solution of 10 mM *N*-Cbz-Gly-OH (MW: 208.07) as the internal standard for MS analysis was made in DMSO.

Resazurin assay.

Stock solutions of CORM-2 and CORM-3 were diluted in DMEM cell culture medium (No. 10-017-CV, Corning Life Sciences) supplemented with 10% fetal bovine serum (FBS) to obtain various concentrations. The resulting solutions were incubated at 37 °C in humidified atmosphere with 5% CO_2 for 24 h. In a 96-well plate, after the incubation, 100 μL solutions of each concentration were added, and then followed by the addition of 20 μL of resazurin sodium salt stock solution (0.15 mg/ml in PBS). The 96-well plate was incubated for additional two hours at 37 °C before measuring the fluorescence at 531 nm excitation and 595 emission using a microplate reader. The negative control group only contained DMEM (10% FBS). The percent deviation value was calculated by the difference between values of the sample and control group, divided by the control value, and multiplied to the percent value.

CCK-8 assay.

Stock solutions of CORM-2 were diluted in DMEM cell culture medium (No. 10-017-CV, Corning Life Sciences) supplemented with 10% fetal bovine serum (FBS) to obtain various concentrations. The resulting solutions were incubated at 37 °C in humidified atmosphere with 5% CO_2 for 24 h to mimic experimental conditions. In a 96-well plate, after the incubation, 100 μL solutions of each concentration were added, and then followed by the addition of 10 μL of CCK-8 (Dojindo, Japan) solution. The plate was incubated for

additional two hours at 37 °C before measuring the optical density at 450 nm with a microplate reader. The negative control group only contained DMEM (10% FBS). Similar to resazurin assay, the percent deviation value was calculated by the difference between values of the sample and control group, divided by the control value, and multiplied to the percent value.

LC-MS analysis of the reaction mixture between CORM-2 and MTT.

MTT (100 μM) or MTT formazan (100 μM) was incubated with 200 μM CORM-2 in PBS (pH 7.4) for 1 h at 37 °C. For analysis, 5 μL of the reaction mixture was injected to the LC-MS system, separated with a C18 column (Phenomenex C18, 3 μm, 3×50 mm) by using gradient eluent (mobile phase: A: H₂O (0.05% FA), B: ACN (0.05% FA). Gradient: 0–2 min 5%B, 2–8 min 5–95% B, 8–9 min (95% B), 9–10 min (5% B). 5 μL of CORM-2 (200 μM), MTT (100 μM), and formazan (100 μM) were also separately injected to serve as controls. The absorbance at 214 nm and 254 nm were monitored by using UV chromatogram. MTT and formazan were detected by using total ion chromatogram (TIC) and extracted ion chromatogram (EIC).

Glutathione (GSH) and GSSG measurements.

To 1 ml of a sample solution containing 100 μM GSSG with or without 100 μM CORM-2 or –3 incubated at 37°C for a designated amount of time (2 or 18 h), 10 μL of a mBBR stock solution was added. The resulting mixture was incubated for 30 min at 37 °C before measuring the fluorescence at 390 nm excitation and 482 emission on a fluorometer. For quantifications of GSH and GSSG, the sample was analyzed by LC-MS. Generally, 1 μL of the internal standard (IS) stock solution was added to 200 μL of the control or the reaction mixture. The mixture was vortexed for 10 s and 10 μL was injected to the LC-MS system, separated with C18 column (Kromasil, 3.5 μm, 4.6×150 mm or Waters Sunfire, 3.5 μm, 3.5×150 mm) by using a gradient eluent (ACN:H₂O with 0.1% FA, 2%–95% in 10 min, 0.7 ml/min). The extracted molecular ion peaks of the GSSG ($m/z=611$, [M-H]⁻), GSH-bimane ($m/z=496$, [M-H]⁻), and the internal standard ($m/z=208$, [M-H]⁻) were detected under negative ion mode and integrated using default settings. Semi-quantitative determination of GSSG decrease was made by directly comparing the ratio of GSSG/IS. Quantification of GSH-bimane was made by establishing standard curve. To establish a standard curve, 3.125, 6.25, and 12.5 μM GSH in PBS was incubate with mBBR then added with IS before injecting to LCMS.

CO detection by gas chromatography (GC).

1 ml of various reaction solutions was prepared and immediately charged in a 2-ml headspace vial (27058, Sigma-Aldrich) capped with an aluminum seal with PTFE/rubber liner (27102-U, Sigma-Aldrich). The reaction solutions were incubated at 37 °C for 14 h to allow CO release. For a CO gas control, 40 μL of pure CO gas (Airgas) was injected into the headspace of a sealed 2-ml vial containing the same solvent. The CO gas control was also incubated at 37°C for 24 h before GC analysis. For each reaction mixture or the CO gas control, 250 μL of gas sample was taken from the headspace by a gas-tight syringe (Hamilton®). The gas sample was analyzed by a GC system with TCD detection. Helium was used as the carrier gas with a flow rate of 30 mL/min. Gaseous components of the

headspace were separated by passing through a packed column (60/80 Carboxen-1000 matrix support, L×O.D.×I.D. 15.0 ft (4.6 m) × 1/8 in × 2.1 mm, Supelco). The column was heated to 35 °C for 5 min, and then the column temperature was increased to 225 °C at a rate of 20 °C/min while the detector temperature was held at 125 °C.

Griess test.

Nitrite concentrations were measured by the Griess method. According to the vendor's procedure, 50 µL sample solution was mixed with 25 µL Griess reagent R1 (No. 780018, Cayman Chemical) and 25 µL Griess reagent R2 (No. 780020, Cayman Chemical). The resulting mixture was incubated for 10 min before measuring the absorbance at 530 nm. The nitrite concentrations were quantified by using a standard curve.

CO gas treatment.

To a 6-ml headspace vial, 2 ml of the sample solution was added. 1 to 10 ml of pure CO gas (Airgas) was directly bubbled into the solution by a headspace gas syringe. The resulting solution was further incubated under various conditions followed by acquisition of the spectroscopic spectra.

RESULTS AND DISCUSSION

Resazurin (Alamar Blue) is an *N*-oxide-based dye, widely used in cytotoxicity studies for measuring mammalian cell viability and mitochondrial activity.^{57–59} The blue and weakly fluorescent resazurin can be intracellularly reduced to a pink and highly fluorescent compound, resorufin, in metabolically active cells (Figure 3A). In CO and CO-RMs related studies, the resazurin reduction assay has been used to evaluate cytotoxicity.^{33, 57} Previously, we reported that CORM-2 and CORM-3 could directly reduce the aromatic nitro group to an amino group under physiological conditions.⁴¹ We wonder whether ruthenium-based CO-RMs would also lead to the reduction of *N*-oxide compounds, such as resazurin. If so, such property could affect the design of experiments using resazurin as an indicator of cell viability, when CORM-2 or CORM-3 is present.

To test the reactivity of ruthenium-based CO-RMs with resazurin, we first incubated 5 µM of resazurin with 50 µM of CORM-2 or CORM-3 individually in PBS. In both cases, the fluorescence signal at around 583 nm showed a significant increase within an hour (Figure 3B, 3C), and the color of the solution changed from blue to pink, corresponding to the formation of resorufin (Figure 3A). Such changes were also dependent on the concentration of CORM-2 and CORM-3 from 0 to 50 µM (Figure 3D and 3E). Under the same conditions, resazurin was also treated with the inactive forms of CO-RMs, iCORM-2 and iCORM-3, neither of which significantly affected the fluorescence upon incubation with resazurin in PBS for 1 h (Figure 3F, S2). For additional control studies, we also injected 10 ml pure CO gas into the resazurin solution in a sealed vial to see whether CO alone would lead to such a reduction reaction; no change in fluorescence was observed (Figure 3F, S2). To examine the possible reactivity from the combination of iCORMs and CO, pure CO gas was injected together with iCORM-2 or iCORM-3 into the resazurin solution. The iCORM-3 and CO combination did not generate any fluorescent change either (Figure S3). Interestingly,

iCORM-2 and CO gas together led to fluorescence turn-on of resazurin (Figure S3). This might suggest the catalytic role of the ruthenium core in iCORM-2, which mediates the reduction of resazurin in the presence of CO. However, to fully understand the intricate details of the mechanism as to why CORM-2 and -3 are different, much more additional chemistry work would be needed. We also examined the reactivities of other non-ruthenium CO-RMs and organic CO prodrugs toward resazurin. Manganese- and a boron-based CORMs, namely CORM-401 and CORM-A1 (Figure 1), did not lead to any change in fluorescence of the resazurin solution (Figure 3F, S2). Organic CO prodrugs, **CO-103**²⁷ and **CO-111**,⁵⁵ did not lead to an increase in fluorescent signal either, indicating a lack of chemical reaction with resazurin (Figure S4). The above results indicate a mechanism for the reduction of resazurin to resorufin by ruthenium-based CO-RMs, which is dependent on its intrinsic chemical reactivity.

Another widely used cell proliferation and cytotoxicity assay is based on tetrazolium salts, which can be reduced by cellular reductase to produce the strongly colored formazan products. Among various tetrazolium salts, MTT (3-(4,5-dimethylthiazol-2-yl)-2,5-diphenyltetrazolium bromide) is the most commonly used agent, which was introduced by Mosmann nearly two decades ago.⁶⁰ In live cells, MTT is reduced by cytoplasmic or mitochondrial reductases to form the insoluble purple MTT formazan. Therefore, an increase in absorbance between 550–600 nm is proportional to cell viability. The MTT assay has also been used in studies of CO and CO donors.^{61–68} With the discovery of the reducing activities of ruthenium-based CO-RMs toward aromatic nitro compound and resazurin, we also ask the question of whether there is any interaction between MTT and ruthenium-based CO-RMs.

As an initial test, we simply mixed CORM-2 or CORM-3 with an MTT solution and observed almost instantaneous color change from yellow to dark purple. Such a phenomenon is very similar to what is expected from MTT reduction through cellular respiration. Therefore, we conducted further characterizations by using UV spectroscopy. 100 μM of MTT shows a distinct absorption at around 400 nm in PBS solution (Figure 4A). Upon the addition of two equivalents of CORM-2 or CORM-3, a new absorption peak at around 600 nm formed, corresponding to the visible purple color (Figure 4A). As control experiments, we also incubated CO-depleted iCORM-2 or iCORM-3 with MTT under the same conditions. However, we did not observe any absorption change above 500 nm (Figure 4A). As a second control study, we added CO gas to the mixture of iCORMs (iCORM-2 or iCORM-3) and MTT to mimic the released products from CORM-2 and CORM-3. The combination of iCORM-3 and CO gas did not lead to UV absorption change (Figure S5). In contrast, 1 ml of pure CO gas caused a slight increase in absorption at around 600 nm (Figure S6) when added to the mixture of iCORM-2 and MTT. However, this change was much smaller than that caused by CORM-2. We also treated MTT with other CO-RMs (CORM-A1 and CORM-401) and did not observe any spectroscopic changes (Figure S7).

To examine whether the color change of MTT caused by ruthenium-based CO-RMs was due to MTT formazan production, the mixture of CORM-2 and MTT in DSMS- d_6 (10% PBS) was monitored by ¹H-NMR. Interestingly, the chemical shift of MTT did not show any difference after incubating with CORM-2 (Figure S8), although the corresponding color

change was observed. We also compared the UV spectrum of the MTT-CORM-2 mixture with that of MTT formazan, and observed some differences in UV absorbance patterns (Figure S9). As such, the reaction mixture of MTT and CORM-2 was further analyzed by LC-MS. Upon incubation of MTT (100 μM) with CORM-2 (200 μM) for 1 h in PBS at 37 $^{\circ}\text{C}$, in the chromatogram monitored by UV at 254 nm, the peak of MTT disappeared without the observation of a peak corresponding to formazan (Figure S10). In the LC-MS chromatogram based on ion flux, multiple peaks corresponding to the molecular weight of MTT or formazan were detected at various retention times, indicating the formation of several complexes/adducts during the incubation of MTT with CORM-2 (Figure S11) and the complexity of the chemistry. These adducts might collapse during the chromatographic and/or ionization process, leading to the different retention times for what appeared to be MTT or formazan. In the LC-MS chromatogram of the reaction mixture, the appearance of a peak corresponding to both the retention time and the molecular weight of formazan indicates the ability for CORM-2 to reduce MTT, though not to a significant extent that is measurable by NMR or UV (Figure S12). Incubation of formazan (100 μM) with CORM-2 (200 μM) also led to a change in the formazan peak in the UV chromatogram, suggesting possible interaction between formazan and CORM-2 (Figure S12). There are earlier literature reports that tetrazole and formazan are able to chelate to ruthenium (II),^{69, 70} which might explain the spectroscopic changes observed. For the next step, we also studied the UV spectroscopic changes of MTT formazan when treated with CORM-2 and CORM-3. As shown in Figure S13, in the presence of 100 μM of CORM-2, the peak intensity of MTT formazan gradually decreased. At the 50-min time point, the peak at 600 nm disappeared almost completely. 100 μM of CORM-3 also led to the disappearance of the peak corresponding to MTT formazan within 1 h (Figure S14). Additionally, we also used iCORM-2 and iCORM-3 in control studies. iCORM-2 also led to a decrease of the MTT formazan absorption peak. However, the effect was only 40% of that of CORM-2 at the 90-min time point (Figure S15). iCORM-3, on the other hand, induced spectroscopic changes of MTT formazan to the same magnitude as that of CORM-3 (Figure S16). The perturbation of the spectroscopic properties of MTT and MTT formazan is something that needs to be carefully considered in designing future experiments using CORM-2 and CORM-3 when MTT is used in cytotoxicity studies.

Ruthenium-based CO-RMs have also been tested with another commonly used water-soluble tetrazolium compound, WST-8, which is the active ingredient in the commonly used CCK-8 assay. Similar to MTT, WST-8 also serves as a redox indicator to represent cell viability and has been widely used in CORM-based cytotoxicity studies.^{71–75} Upon addition of 100 μM of CORM-2 or CORM-3 to WST-8 in PBS, a new peak at 450 nm appeared within 30 min of incubation at 37 $^{\circ}\text{C}$ (Figure 4B). However, inactive forms of CORM-2 and CORM-3, iCORM-2 and iCORM-3 failed to produce any response under the same conditions (Figure 4B). It should be noted that the readouts from CCK-8 is based on the absorbance change of WST-8 at 460 nm in a generally accepted protocol. As such, the spectroscopic changes caused by CORM-2 and CORM-3 are factors to consider when designing future experiments involving CCK-8.

For cytotoxicity studies by using resazurin- and MTT-based assays, CORM-2 and -3 were normally incubated with cells in culture medium for 24 h before performing the assays.

^{33, 76–79} To mimic such a process, we preincubated various concentrations (used in previous studies) of CORM-2 and -3 in DMEM (10% FBS) for 24 h at 37 °C. Then, resazurin and CCK-8 assays were conducted, and the readouts were compared to that from the respective control group. The results are presented in the format to show deviations from the control group. In the presence of CORM-2 within a concentration range seen in the literature (50 to 500 μM), the deviations from the respective controls were determined to be in the range of 3% to 35% with a dose-dependent effect in the CCK-8 assay (Figure 5A). For the resazurin assay, CORM-2 also caused a dose-dependent increase. With increasing CORM-2 concentrations from 50 to 500 μM, the deviation percentage elevated by over 3 fold (Figure 5B). A similar dose-dependent pattern was also observed when applying CORM-3 to the resazurin and CCK-8 assays. The highest concentration (1 mM) of CORM-3 led to around 55% and 33% deviations in the CCK-8 and resazurin assay, respectively (Figure S17). No significant deviation was found in the presence of CORM-3 at a lower concentration (50 and 100 μM) in the resazurin assay (Figure S17B). These results indicate that pre-incubation of ruthenium-based CO-RMs in cell culture medium could diminish their interfering effects toward resazurin and CCK-8 assays. However, because of the concentration-dependent nature of the effects, it is suggested that one takes into consideration of all these factors and concentration range in designing experiments that use the CCK-8 and resazurin assays.

CORM-2 and CORM-3 have been extensively reported to inhibit NO production triggered by various inflammatory stimulators *in vivo*.^{80, 81} A previous study showed the ability for CORM-2 to directly quench NO released from a NO donor (diethylamine NONOate) *in vitro*.⁴⁸ Due to the rapid oxidation of NO to nitrite by oxygen, the NO concentration in biological studies is usually determined by measuring its nitrite content as a surrogate. Acting as reducing agents to both aryl nitro and *N*-oxide groups, we are interested in evaluating if CORM-2 and -3 can also directly react with nitrite, which is the key analyte/ingredient for determining NO concentration. To start with, 100 μM of nitrite was incubated with CORM-2 in PBS for 5 h and 24 h at 37 °C, followed by determining the nitrite concentration using the Griess test. To our surprise, 50 and 100 μM CORM-2 dropped the nitrite concentration by 14% and 15% at the 5-h point and 21% and 34% at the 24-h point, respectively (Figure 6A, S18A). iCORM-2 also caused a comparable decrease in nitrite concentration. 100 μM iCORM-2 decreased the nitrite concentration by almost 48% after 24 h of incubation, which was even lower than that caused by CORM-2 (Figure 7A). CORM-3 was also examined under the same conditions. Upon treatment with 100 μM of CORM-3 for 5 h and 24 h, the nitrite concentration was reduced by 14% and 38%, respectively (Figure 6B, S18B). Under the same conditions, iCORM-3 did not lead to a significant decrease after 5 h of treatment; however, at the 24-h point, the nitrite concentration decreased by 22%. Such results suggest a weaker reactivity of iCORM-3 compared with CORM-3 (Figure S18B). Our results indicate that both CORM-2 and CORM-3 directly consume nitrite *in vitro*. There are several implications of these results. First, iCORM-2 and iCORM-3 may not be considered as suitable controls for CORM-2,3 in studying the effect of CO on NO production. Second, given the ability for CORM-2,3 and iCORM-2,3 to directly react with nitrite, their ability to directly perturb cellular redox balance may need to be considered when CORM-2,3 are used to study the effect of CO on attenuating redox stress.

Activated azido groups are known to be reduced by H₂S, and such reactivity is widely used in designing H₂S fluorescent probes.^{56, 82, 83} Both of DNS-Az⁵⁶ and AzMC⁸⁴ are H₂S fluorescent probes bearing an azido group attached to a fluorophore (Figure 7A, 8A). The reduction of such an azido group to the corresponding amino group by H₂S is the basis for fluorescence turn-on and thus sulfide detection. We were interested in seeing if ruthenium-based CO-RMs could reduce these probes. Therefore, we first studied the response from DNS-Az in the presence of CORM-2. Upon incubation with 100 μM of CORM-2 in PBS/ACN (1:1), the fluorescence intensity of DNS-Az significantly increased within the first 20 min to reach a plateau (Figure S19). Concentration-dependent fluorescence intensity changes were also observed in the presence of 20 to 100 μM CORM-2 (Figure 7B). Incubations with either iCORM-2 or CO gas did not lead to any fluorescence changes (Figure 7B). 100 μM of CORM-3 also caused an increase in fluorescence intensity of the DNS-Az solution within 20 min, while iCORM-3 did not show any reactivity (Figure 7D, S20). Next, AzMC was tested with CORM-2 and CORM-3. Both CORM-2 and CORM-3 led to an increase of the fluorescence intensity of AzMC within 1 h of incubation at room temperature, while incubation with iCORM-2 and iCORM-3 resulted in minimal increases in the fluorescent intensity (Figure 8, S21). These results suggest that CORM-2 and CORM-3 are capable of reducing the azido groups presented in two representative H₂S probes, DNS-Az and AzMC, while iCORM-2/3 failed to do so.

GSH and GSSG are known to be important regulators in cellular redox signaling.^{85, 86} The redox conversion between GSSG and GSH are dynamically modulated under various oxidative conditions.⁸⁷ As such, the ratio of GSH/GSSG is normally used as an indicator of cellular redox status.⁸⁶ More importantly changes in the levels of GSH and GSSG are associated with many essential biological processes, such as apoptosis and growth stimulation.⁸⁸ One of the mechanisms through which CO has been reported to exert its cytoprotection action is through the modulation of cellular redox chemistry.⁸⁹ Previous studies have revealed the redox activity of Ru-based CO-RMs themselves^{31, 37, 41} and the ability to react with thiols,^{19, 32, 39} which are important players in modulating cellular redox signaling. Therefore, we are interested in examining the effects of CORM-2 and -3 on GSSG in the context of redox chemistry, i.e. the ability to reduce GSSG to GSH. To start with, 100 μM of CORM-2 was incubated with GSSG (100 μM) in PBS (pH = 7.4) at 37 °C for 2 h. Then mBBR (final conc. 1 mM) was added to trap the generated GSH as a fluorescent adduct (experimental section).⁹⁰ As compared to the individual GSSG and CORM-2 control groups, the fluorescence intensity at 482 nm showed a significant increase in the CORM-2/GSSG reaction group (Figure S22). Such results indicate the ability for CORM-2 to reduce GSSG to GSH. After incubating 100 μM GSSG with 100 μM CORM-2 for 2 h, the formation of GSH in the BBr trapped form was confirmed and measured to be 5.5 μM by LC-MS analysis (Figure S23, Table S1). Furthermore, LC-MS also confirmed that GSSG decreased by about 70% with formation of several unidentified products after incubating with 100 μM CORM-2 for 18 h (Table S2, Figure S24). Similarly, CORM-3 also decreased GSSG concentration by about 30% after 18 h of incubation, less than that with CORM-2 (Table S3). Increased GSSG/GSH ratios and protein glutathionylation have been found in cells from patients with cancer and neurological disorders, or under chemically induced oxidative stress.^{91–94} As such, the redox properties of CORM-2, -3 and their ability to reduce GSSG are factors to

consider in conducting pharmacological studies using these two CO-RMs, especially in studying CO-mediated redox signaling. Additionally, CO release from CORM-2 was also monitored in the presence of GSH or GSSG by GC-TCD chromatography (See experimental section for details). In the headspace of CORM-2 (2 mM, 1 ml) PBS/DMSO (1:1) solution, not CO, but CO₂ was found to be the major product from CORM-2 (Figure S25). This observation is consistent with the findings from earlier reports,³¹ indicating the water-gas-shift was the dominant reaction in the CORM-2 aqueous solution. Interestingly, in the presence of GSH (4 mM), but not GSSG (2 mM), we observed a prominent CO peak and a decreased level of CO₂ peak in GC (Figure S25). However, such a CO peak is much smaller than that in the CO gas control (~2 μmol CO, 1 equiv. of CORM-2). These results indicate the reactivity of CORM-2 towards GSH might help CO generation in aqueous environments and support the notion that CORM-2 undergoes extensive chemical reactions with species present in biological milieu.

CONCLUSION

In this work, we report the intrinsic reactivities of ruthenium-based CO-RMs including: i) reduction of resazurin; ii) perturbation of the spectroscopic properties of tetrazolium salts, MTT and WST-8; iii) consumption of nitrites *in vitro*; iv) reduction of azide-based H₂S fluorescent probes, DNS-Az and AzMc; and v) consumption and reduction of GSSG. All of these reagents are highly relevant to assessing CO's biological effects. Because of the large number of biological effects that have been reported for CO, including redox signaling, cytoprotection, anti-inflammation, and cross-talks with sulfide- and NO-mediated signaling, the implications of the described chemical reactivity of CORM-2,3 are convoluted. Obviously, caution is needed in extrapolating the solution-phase studies to cellular and animal model studies, because of the increased levels of complexity when it goes beyond controlled solution-phase studies. The chemical studies described do not allow us to draw any conclusion on the impact of such reactivities on specific biological studies, especially in animal models. However, findings from such studies indeed provide very important factors to consider when designing future experiments involving CORM-2 and -3 and the reagents studied.

Supplementary Material

Refer to Web version on PubMed Central for supplementary material.

ACKNOWLEDGMENT

We gratefully acknowledge the financial support by the National Institutes of Health (R01DK119202) for our CO related work, the Georgia Research Alliance for an Eminent Scholar endowment, the Brains & Behaviors program for a graduate fellowship to ZY, and internal resources at Georgia State University. We would also like to thank Professor Leo Otterbein of Beth Israel Deaconess Medical Center/Harvard Medical School for his valuable suggestions.

REFERENCES

1. Wu L; Wang R, Carbon monoxide: endogenous production, physiological functions, and pharmacological applications. *Pharmacol. Rev* 2005, 57, 585–630. [PubMed: 16382109]

2. Motterlini R; Otterbein LE, The therapeutic potential of carbon monoxide. *Nat. Rev. Drug Discov* 2010, 9, 728–743. [PubMed: 20811383]
3. Tayem Y; Johnson TR; Mann BE; Green CJ; Motterlini R, Protection against cisplatin-induced nephrotoxicity by a carbon monoxide-releasing molecule. *Am. J. Physiol. Renal Physiol* 2006, 290 (4), F789–F794. [PubMed: 16291575]
4. Steiger C; Uchiyama K; Takagi T; Mizushima K; Higashimura Y; Gutmann M; Hermann C; Botov S; Schmalz H-G; Naito Y; Meinel L, Prevention of colitis by controlled oral drug delivery of carbon monoxide. *J. Control. Release* 2016, 239, 128–136. [PubMed: 27578097]
5. Hoetzel A; Dolinay T; Schmidt R; Choi AMK; Ryter SW, Carbon Monoxide in Sepsis. *Antioxid. Redox Signal* 2007, 9 (11), 2013–2026. [PubMed: 17822362]
6. Bakalarz D; Surmiak M; Yang X; Wójcik D; Korbut E; Iliwowski Z; Ginter G; Buszewicz G; Brzozowski T; Cieszkowski J; Głowacka U; Magierowska K; Pan Z; Wang B; Magierowski M, Organic carbon monoxide prodrug, BW-CO-111, in protection against chemical-induced gastric mucosal damage. *Acta Pharm. Sin. B* 2020, in press.
7. Yang X; de Caestecker M; Otterbein LE; Wang B, Carbon monoxide: An emerging therapy for acute kidney injury. *Med. Res. Rev* 2019, 40 (4), 1147–1177. [PubMed: 31820474]
8. Ji X; Damera K; Zheng Y; Yu B; Otterbein LE; Wang B, Toward CO-based Therapeutics: Critical Drug Delivery and Developability Issues. *J. Pharm. Sci* 2016, 105, 405–416 and references cited therein.
9. Soboleva T; Esquer HJ; Anderson SN; Berreau LM; Benninghoff AD, Mitochondrial-Localized Versus Cytosolic Intracellular CO-Releasing Organic PhotoCORMs: Evaluation of CO Effects Using Bioenergetics. *ACS Chem. Biol* 2018, 13, 2220–2228. [PubMed: 29932318]
10. Soboleva T; Simons CR; Arcidiacono A; Benninghoff AD; Berreau LM, Extracellular vs Intracellular Delivery of CO: Does It Matter for a Stable, Diffusible Gasotransmitter? *J Med Chem* 2019, 62, 9990–9995. [PubMed: 31577143]
11. Zheng Y; Ji X; Yu B; Ji K; Gallo D; Csizmadia E; Zhu M; de la Cruz LKC; Choudhary MR; Chittavong V; Pan Z; Yuan Z; Otterbein LE; Wang B, Enrichment-triggered Prodrug Activation Demonstrated through Mitochondria-targeted Delivery of Doxorubicin and Carbon Monoxide. *Nat. Chem* 2018, 10, 787–794. [PubMed: 29760413]
12. Clark James E; Naughton P; Shurey S; Green Colin J; Johnson Tony R; Mann Brian E; Foresti R; Motterlini R, Cardioprotective Actions by a Water-Soluble Carbon Monoxide-Releasing Molecule. *Circ. Res* 2003, 93 (2), e2–e8. [PubMed: 12842916]
13. Crook SH; Mann BE; Meijer AJHM; Adams H; Sawle P; Scapens D; Motterlini R, $[\text{Mn}(\text{CO})_4\{\text{S}2\text{CNMe}(\text{CH}_2\text{CO}_2\text{H})\}]$, a new water-soluble CO-releasing molecule. *Dalton Trans.* 2011, 40 (16), 4230–4235. [PubMed: 21403944]
14. Mann BE, CO-Releasing Molecules: A Personal View. *Organometallics* 2012, 31, 5728–5735.
15. Motterlini R; Clark James E; Foresti R; Sarathchandra P; Mann Brian E; Green Colin J, Carbon Monoxide-Releasing Molecules. *Circ. Res* 2002, 90 (2), e17–e24. [PubMed: 11834719]
16. Heinemann SH; Hoshi T; Westerhausen M; Schiller A, Carbon monoxide--physiology, detection and controlled release. *Chem. Commun* 2014, 50 (28), 3644–60.
17. Carrington SJ; Chakraborty I; Bernard JM; Mascharak PK, Synthesis and Characterization of a “Turn-On” photoCORM for Trackable CO Delivery to Biological Targets. *ACS Med. Chem. Lett* 2014, 5, 1324–8. [PubMed: 25516792]
18. Romão CC; Blättler WA; Seixas JD; Bernardes GJ, Developing drug molecules for therapy with carbon monoxide. *Chem. Soc. Rev* 2012, 41, 3571–83. [PubMed: 22349541]
19. Santos-Silva T; Mukhopadhyay A; Seixas JD; Bernardes GJ; Romão CC; Romão MJ, Towards improved therapeutic CORMs: understanding the reactivity of CORM-3 with proteins. *Curr. Med. Chem* 2011, 18, 3361–6. [PubMed: 21728965]
20. Popova M; Soboleva T; Ayad S; Benninghoff AD; Berreau LM, Visible-Light-Activated Quinolone Carbon Monoxide-Releasing Molecule: Prodrug and Albumin-Assisted Delivery Enables Anticancer and Potent Anti-Inflammatory Effects. *J. Am. Chem. Soc* 2018, 140 (30), 9721–9729. [PubMed: 29983046]
21. Soboleva T; Berreau LM, 3-Hydroxyflavones and 3-Hydroxy-4-oxoquinolines as Carbon Monoxide-Releasing Molecules. *Molecules* 2019, 24, 1252.

22. Soboleva T; Esquer HJ; Benninghoff AD; Berreau LM, Sense and Release: A Thiol-Responsive Flavonol-Based Photonicallly Driven Carbon Monoxide-Releasing Molecule That Operates via a Multiple-Input AND Logic Gate. *J Am Chem Soc* 2017, 139 (28), 9435–9438. [PubMed: 28677975]
23. Peng P; Wang C; Shi Z; Johns VK; Ma L; Oyer J; Copik A; Igarashi R; Liao Y, Visible-light activatable organic CO-releasing molecules (PhotoCORMs) that simultaneously generate fluorophores. *Org. Biomol. Chem* 2013, 11 (39), 6671–4. [PubMed: 23943038]
24. Palao E; Slanina T; Muchova L; Solomek T; Vitek L; Klan P, Transition-Metal-Free CO-Releasing BODIPY Derivatives Activatable by Visible to NIR Light as Promising Bioactive Molecules. *J. Am. Chem. Soc* 2016, 138 (1), 126–33. [PubMed: 26697725]
25. Urdabayev NK; Poloukhine A; Popik VV, Two-photon induced photodecarbonylation reaction of cyclopropanones. *Chem. Commun* 2006, 454–6.
26. Antony LA; Slanina T; Šebej P; Šolomek T; Klán P, Fluorescein analogue xanthene-9-carboxylic acid: a transition-metal-free CO releasing molecule activated by green light. *Org. Lett* 2013, 15, 4552–5. [PubMed: 23957602]
27. Ji X; Zhou C; Ji K; Aghoghovbia RE; Pan Z; Chittavong V; Ke B; Wang B, Click and Release: A Chemical Strategy toward Developing Gasotransmitter Prodrugs by Using an Intramolecular Diels–Alder Reaction. *Angew. Chem. Int. Ed* 2016, 55 (51), 15846–15851.
28. Ji X; Pan Z; Li C; Kang T; De La Cruz LKC; Yang L; Yuan Z; Ke B; Wang B, Esterase-Sensitive and pH-Controlled Carbon Monoxide Prodrugs for Treating Systemic Inflammation. *J. Med. Chem* 2019, 62 (6), 3163–3168. [PubMed: 30816714]
29. Ji X; Wang B, Strategies toward Organic Carbon Monoxide Prodrugs. *Acc. Chem. Res* 2018, 51, 1377–1385. [PubMed: 29762011]
30. Kueh JTB; Stanley NJ; Hewitt RJ; Woods LM; Larsen L; Harrison JC; Rennison D; Brimble MA; Sammut IA; Larsen DS, Norborn-2-en-7-ones as physiologically-triggered carbon monoxide-releasing prodrugs. *Chem. Sci* 2017, 8 (8), 5454–5459. [PubMed: 28970925]
31. Seixas JD; Santos MFA; Mukhopadhyay A; Coelho AC; Reis PM; Veiros LF; Marques AR; Penacho N; Gonçalves AML; Romão MJ; Bernardes GJL; Santos-Silva T; Romão CC, A contribution to the rational design of Ru(CO)₃Cl₂L complexes for in vivo delivery of CO. *Dalton Trans.* 2015, 44 (11), 5058–5075. [PubMed: 25427784]
32. Southam HM; Smith TW; Lyon RL; Liao C; Trevitt CR; Middlemiss LA; Cox FL; Chapman JA; El-Khamisy SF; Hippler M; Williamson MP; Henderson PJF; Poole RK, A thiol-reactive Ru(II) ion, not CO release, underlies the potent antimicrobial and cytotoxic properties of CO-releasing molecule-3. *Redox Biol.* 2018, 18, 114–123. [PubMed: 30007887]
33. Juszczak M; Kluska M; Wysoki ski D; Wo niak K, DNA damage and antioxidant properties of CORM-2 in normal and cancer cells. *Sci Rep* 2020, 10, 12200. [PubMed: 32699258]
34. Nielsen VG, The anticoagulant effect of *Apis mellifera* phospholipase A(2) is inhibited by CORM-2 via a carbon monoxide-independent mechanism. *J Thromb. Thrombolysis* 2020, 49, 100–107. [PubMed: 31679116]
35. Nielsen VG; Wagner MT; Frank N, Mechanisms Responsible for the Anticoagulant Properties of Neurotoxic Dendroaspis Venoms: A Viscoelastic Analysis. *Int. J. Mol. Sci* 2020, 21 (6), 2082.
36. Nielsen VG, Ruthenium, Not Carbon Monoxide, Inhibits the Procoagulant Activity of Atheris, Echis, and Pseudonaja Venoms. *Int. J. Mol. Sci* 2020, 21 (8), 2970.
37. Stucki D; Krahl H; Walter M; Steinhausen J; Hommel K; Brenneisen P; Stahl W, Effects of frequently applied carbon monoxide releasing molecules (CORMs) in typical CO-sensitive model systems - A comparative in vitro study. *Arch. Biochem. Biophys* 2020, 687, 108383. [PubMed: 32335048]
38. Rossier J; Delasoie J; Haeni L; Hauser D; Rothen-Rutishauser B; Zobi F, Cytotoxicity of Mn-based photoCORMs of ethynyl- α -diimine ligands against different cancer cell lines: The key role of CO-depleted metal fragments. *J. Inorg. Biochem* 2020, 209, 111122. [PubMed: 32497818]
39. Santos-Silva T; Mukhopadhyay A; Seixas JD; Bernardes GJ; Romão CC; Romão MJ, CORM-3 reactivity toward proteins: the crystal structure of a Ru(II) dicarbonyl-lysozyme complex. *J. Am. Chem. Soc* 2011, 133 (5), 1192–5. [PubMed: 21204537]

40. Nobre LS; Jeremias H; Romao CC; Saraiva LM, Examining the antimicrobial activity and toxicity to animal cells of different types of CO-releasing molecules. *Dalton Trans.* 2016, 45 (4), 1455–1466. [PubMed: 26673556]
41. Yuan Z; Yang X; De La Cruz LKC; Wang B, Nitro reduction-based fluorescent probes for carbon monoxide require reactivity involving a ruthenium carbonyl moiety. *Chem. Commun* 2020, 56 (14), 2190–2193.
42. Wareham LK; Poole RK; Tinajero-Trejo M, CO-releasing metal carbonyl compounds as antimicrobial agents in the post-antibiotic era. *J. Biol. Chem* 2015, 290 (31), 18999–19007. [PubMed: 26055702]
43. Gessner G; Sahoo N; Swain SM; Hirth G; Schönherr R; Mede R; Westerhausen M; Brewitz HH; Heimer P; Imhof D; Hoshi T; Heinemann SH, CO-independent modification of K(+) channels by tricarbonyldichlororuthenium(II) dimer (CORM-2). *Eur. J. Pharmacol* 2017, 815, 33–41. [PubMed: 28987271]
44. Dong DL; Chen C; Huang W; Chen Y; Zhang XL; Li Z; Li Y; Yang BF, Tricarbonyldichlororuthenium (II) dimer (CORM2) activates non-selective cation current in human endothelial cells independently of carbon monoxide releasing. *Eur. J. Pharmacol* 2008, 590 (1–3), 99–104. [PubMed: 18582862]
45. Nielsen VG; Garza JI, Comparison of the effects of CORM-2, CORM-3 and CORM-A1 on coagulation in human plasma. *Blood Coagul. Fibrinolysis* 2014, 25 (8), 801–5.
46. Johnson TR; Mann BE; Teasdale IP; Adams H; Foresti R; Green CJ; Motterlini R, Metal carbonyls as pharmaceuticals? [Ru(CO)₃Cl(glycinate)], a CO-releasing molecule with an extensive aqueous solution chemistry. *Dalton Trans* 2007, 1500–8. [PubMed: 17404651]
47. Funaioli T; Cavazza C; Marchetti F; Fachinetti G, Aqueous Organometallic Chemistry of Ruthenium(II). *Aquo Carbonyl Derivatives and Related Ethene Hydrocarboxylation in Fully Aqueous Solvent.* *Inorg. Chem* 1999, 38 (14), 3361–3368. [PubMed: 11671072]
48. Marazioti A; Bucci M; Coletta C; Vellecco V; Baskaran P; Szabó C; Cirino G; Marques Ana R; Guerreiro B; Gonçalves Ana ML; Seixas João D; Beuve A; Romão Carlos C; Papapetropoulos A, Inhibition of Nitric Oxide–Stimulated Vasorelaxation by Carbon Monoxide-Releasing Molecules. *Arterioscler. Thromb. Vasc. Biol* 2011, 31 (11), 2570–2576.
49. Casey CP; Bikzhanova GA; Cui Q; Guzei IA, Reduction of Imines by Hydroxycyclopentadienyl Ruthenium Hydride: Intramolecular Trapping Evidence for Hydride and Proton Transfer Outside the Coordination Sphere of the Metal. *J. Am. Chem. Soc* 2005, 127 (40), 14062–14071. [PubMed: 16201828]
50. Nomura K, Efficient selective reduction of aromatic nitro compounds by ruthenium catalysis under COH₂O conditions. *J. Mol. Catal. A: Chem* 1995, 95 (3), 203–210.
51. Tafesh AM; Weiguny J, A Review of the Selective Catalytic Reduction of Aromatic Nitro Compounds into Aromatic Amines, Isocyanates, Carbamates, and Ureas Using CO. *Chem. Rev* 1996, 96 (6), 2035–2052. [PubMed: 11848820]
52. Calabrese G; Morgan B; Riemer J, Mitochondrial Glutathione: Regulation and Functions. *Antioxid Redox Signal* 2017, 27, 1162–1177. [PubMed: 28558477]
53. Mailloux RJ, Protein S-glutathionylation reactions as a global inhibitor of cell metabolism for the desensitization of hydrogen peroxide signals. *Redox Biol* 2020, 32, 101472. [PubMed: 32171726]
54. Babu D; Leclercq G; Motterlini R; Lefebvre R, Differential effects of CORM-2 and CORM-401 in murine intestinal epithelial MODE-K cells under oxidative stress. *Front. Pharmacol* 2017, 8, 31. [PubMed: 28228725]
55. Pan Z; Chittavong V; Li W; Zhang J; Ji K; Zhu M; Ji X; Wang B, Organic CO Prodrugs: Structure–CO-Release Rate Relationship Studies. *Chem. Eur. J* 2017, 23 (41), 9838–9845. [PubMed: 28544290]
56. Peng H; Cheng Y; Dai C; King AL; Predmore BL; Lefer DJ; Wang B, A Fluorescent Probe for Fast and Quantitative Detection of Hydrogen Sulfide in Blood. *Angew. Chem. Intl. Ed* 2011, 50 (41), 9672–9675.
57. O'Brien J; Wilson I; Orton T; Pognan F, Investigation of the Alamar Blue (resazurin) fluorescent dye for the assessment of mammalian cell cytotoxicity. *Eur. J. Biochem* 2000, 267 (17), 5421–5426. [PubMed: 10951200]

58. McMillian MK; Li L; Parker JB; Patel L; Zhong Z; Gunnett JW; Powers WJ; Johnson MD, An improved resazurin-based cytotoxicity assay for hepatic cells. *Cell Biol. Toxicol* 2002, 18 (3), 157–173. [PubMed: 12083422]
59. Abu-Amero KK; Bosley TM, Detection of Mitochondrial Respiratory Dysfunction in Circulating Lymphocytes Using Resazurin. *Archi. Patho. Lab. Med* 2005, 129 (10), 1295–1298.
60. Mosmann T, Rapid colorimetric assay for cellular growth and survival: Application to proliferation and cytotoxicity assays. *J. Immunol. Methods* 1983, 65 (1), 55–63. [PubMed: 6606682]
61. Selvamurugan S; Ramachandran R; Viswanathamurthi P, Ruthenium(II) carbonyl complexes containing S-methylisothiosemicarbazone based tetradentate ligand: synthesis, characterization and biological applications. *Biometals* 2013, 26, 741–53. [PubMed: 23780567]
62. Hettiarachchi NT; Boyle JP; Dallas ML; Al-Owais MM; Scragg JL; Peers C, Heme oxygenase-1 derived carbon monoxide suppresses A β (1–42) toxicity in astrocytes. *Cell Death Dis.* 2017, 8, e2884.
63. Srisook K; Han SS; Choi HS; Li MH; Ueda H; Kim C; Cha YN, CO from enhanced HO activity or from CORM-2 inhibits both O₂- and NO production and downregulates HO-1 expression in LPS-stimulated macrophages. *Biochem. Pharmacol* 2006, 71, 307–18. [PubMed: 16329999]
64. Xu X; Zhang H; Wang K; Tu T; Jiang Y, Protective Effect of Edaravone against Carbon Monoxide Induced Apoptosis in Rat Primary Cultured Astrocytes. *Biochem. Res. Int* 2017, 2017, 5839762. [PubMed: 28261501]
65. Wang P; Liu H; Zhao Q; Chen Y; Liu B; Zhang B; Zheng Q, Syntheses and evaluation of drug-like properties of CO-releasing molecules containing ruthenium and group 6 metal. *Eur. J. Med. Chem* 2014, 74, 199–215. [PubMed: 24463436]
66. Luo X; Zhou X; Su P; Zhu W, [Effects of Scutellaria baicalensis stem-leaf total flavonoid on proliferation of vessel smooth muscle cells stimulated by high triglyceride blood serum]. *Zhongguo Zhong Yao Za Zhi* 2009, 34, 2803–7. [PubMed: 20209920]
67. Upadhyay KK; Jadeja RN; Vyas HS; Pandya B; Joshi A; Vohra A; Thounaojam MC; Martin PM; Bartoli M; Devkar RV, Carbon monoxide releasing molecule-A1 improves nonalcoholic steatohepatitis via Nrf2 activation mediated improvement in oxidative stress and mitochondrial function. *Redox Biol.* 2020, 28, 101314. [PubMed: 31514051]
68. Stamellou E; Storz D; Botov S; Ntasis E; Wedel J; Sollazzo S; Krämer BK; van Son W; Seelen M; Schmalz HG; Schmidt A; Hafner M; Yard BA, Different design of enzyme-triggered CO-releasing molecules (ET-CORMs) reveals quantitative differences in biological activities in terms of toxicity and inflammation. *Redox Biol.* 2014, 2, 739–48. [PubMed: 25009775]
69. Stagni S; Orselli E; Palazzi A; De Cola L; Zacchini S; Femoni C; Marcaccio M; Paolucci F; Zanarini S, Polypyridyl Ruthenium(II) Complexes with Tetrazolate-Based Chelating Ligands. Synthesis, Reactivity, and Electrochemical and Photophysical Properties. *Inorg. Chem* 2007, 46 (22), 9126–9138. [PubMed: 17902649]
70. Jameson GB; Muster A; Robinson SD; Wingfield JN; Ibers JA, Cyclometalated formazan derivatives of ruthenium and osmium: structure of Ru((o-C₆H₄)N:NC(Ph):NNPh)(CO)(PPh₃)₂. *Inorg. Chem* 1981, 20 (8), 2448–2456.
71. Lv C; Su Q; Fang J; Yin H, Styrene-maleic acid copolymer-encapsulated carbon monoxide releasing molecule-2 (SMA/CORM-2) suppresses proliferation, migration and invasion of colorectal cancer cells in vitro and in vivo. *Biochem. Biophys. Res. Commun* 2019, 520, 320–326. [PubMed: 31604526]
72. Pan Y; Song J; Ma L; Zong X; Chen H; Zhao B; Yu Q; Song H, Carbon Monoxide Releasing Molecule 3 Inhibits Osteoclastogenic Differentiation of RAW264.7 Cells by Heme Oxygenase-1. *Cell Physiol. Biochem* 2018, 50, 1988–2003. [PubMed: 30404077]
73. Yoon YE; Lee KS; Lee YJ; Lee HH; Han WK, Renoprotective Effects of Carbon Monoxide-Releasing Molecule 3 in Ischemia-Reperfusion Injury and Cisplatin-Induced Toxicity. *Transplant Proc.* 2017, 49, 1175–1182. [PubMed: 28583551]
74. Shao L; Gu YY; Jiang CH; Liu CY; Lv LP; Liu JN; Zou Y, Carbon monoxide releasing molecule-2 suppresses proliferation, migration, invasion, and promotes apoptosis in non-small cell lung cancer Calu-3 cells. *Eur. Rev. Med. Pharmacol. Sci* 2018, 22, 1948–1957. [PubMed: 29687848]

75. Yan Y; Du C; Li G; Chen L; Yan Y; Chen G; Hu W; Chang L, CO suppresses prostate cancer cell growth by directly targeting LKB1/AMPK/mTOR pathway in vitro and in vivo. *Urol. Oncol* 2018, 36, 312.e1–312.e8.
76. Desmard M; Davidge KS; Bouvet O; Morin D; Roux D; Foresti R; Ricard JD; Denamur E; Poole RK; Montravers P; Morterlini R; Boczkowski J, A carbon monoxide-releasing molecule (CORM-3) exerts bactericidal activity against *Pseudomonas aeruginosa* and improves survival in an animal model of bacteraemia. *FASEB J.* 2009, 23 (4), 1023–1031. [PubMed: 19095732]
77. Wang Y-R; Chen K-L; Li C-M; Li L; Wang G-L, Heme oxygenase 1 regulates apoptosis induced by heat stress in bovine ovarian granulosa cells via the ERK1/2 pathway. *J. Cell. Physiol* 2019, 234 (4), 3961–3972. [PubMed: 30191981]
78. Ma Z; Pu F; Zhang X; Yan Y; Zhao L; Zhang A; Li N; Zhou E-M; Xiao S, Carbon monoxide and biliverdin suppress bovine viral diarrhoea virus replication. *J. Gen. Virol* 2017, 98 (12), 2982–2992. [PubMed: 29087274]
79. Li J; Song L; Hou M; Wang P; Wei L; Song H, Carbon monoxide releasing molecule-3 promotes the osteogenic differentiation of rat bone marrow mesenchymal stem cells by releasing carbon monoxide. *Int J Mol Med* 2018, 41 (4), 2297–2305. [PubMed: 29393384]
80. Choi E-Y; Choe S-H; Hyeon J-Y; Choi J-I; Choi IS; Kim S-J, Carbon monoxide-releasing molecule-3 suppresses *Prevotella intermedia* lipopolysaccharide-induced production of nitric oxide and interleukin-1 β in murine macrophages. *Eur. J. Pharmacol* 2015, 764, 22–29. [PubMed: 26101061]
81. Sun B-W; Sun Y; Sun Z-W; Chen X, CO liberated from CORM-2 modulates the inflammatory response in the liver of thermally injured mice. *World J Gastroenterol* 2008, 14 (4), 547–553. [PubMed: 18203286]
82. Lippert AR; New EJ; Chang CJ, Reaction-Based Fluorescent Probes for Selective Imaging of Hydrogen Sulfide in Living Cells. *J. Am. Chem. Soc* 2011, 133 (26), 10078–10080. [PubMed: 21671682]
83. Wang K; Peng H; Wang B, Recent Advances in Thiol and Sulfide Reactive Probes. *J. Cell. Biochem* 2014, 115 (6), 1007–1022. [PubMed: 24415273]
84. Thorson MK; Majtan T; Kraus JP; Barrios AM, Identification of Cystathionine β -Synthase Inhibitors Using a Hydrogen Sulfide Selective Probe. *Angew. Chem. Intl. Ed* 2013, 52 (17), 4641–4644.
85. Sies H, Glutathione and its role in cellular functions. *Free Radic Biol. Med* 1999, 27 (9), 916–921. [PubMed: 10569624]
86. Schafer FQ; Buettner GR, Redox environment of the cell as viewed through the redox state of the glutathione disulfide/glutathione couple. *Free Radic. Biol. Med* 2001, 30 (11), 1191–1212. [PubMed: 11368918]
87. Xiong Y; Uys JD; Tew KD; Townsend DM, S-glutathionylation: from molecular mechanisms to health outcomes. *Antioxid Redox Signal* 2011, 15 (1), 233–70. [PubMed: 21235352]
88. Kirilin WG; Cai J; Thompson SA; Diaz D; Kavanagh TJ; Jones DP, Glutathione redox potential in response to differentiation and enzyme inducers. *Free Radic. Biol. Med* 1999, 27 (11), 1208–1218. [PubMed: 10641713]
89. Figueiredo-Pereira C; Dias-Pedroso D; Soares NL; Vieira HLA, CO-mediated cytoprotection is dependent on cell metabolism modulation. *Redox Biol.* 2020, 32, 101470. [PubMed: 32120335]
90. Fahey RC; Newton GL; Dorian R; Kosower EM, Analysis of biological thiols: Derivatization with monobromotrimethylammoniumbimane and characterization by electrophoresis and chromatography. *Anal. Biochem* 1980, 107 (1), 1–10. [PubMed: 6449160]
91. Zitka O; Skalickova S; Gumulec J; Masarik M; Adam V; Hubalek J; Trnkova L; Kruseova J; Eckschlager T; Kizek R, Redox status expressed as GSH:GSSG ratio as a marker for oxidative stress in paediatric tumour patients. *Oncol Lett* 2012, 4 (6), 1247–1253. [PubMed: 23205122]
92. James SJ; Rose S; Melnyk S; Jernigan S; Blossom S; Pavliv O; Gaylor DW, Cellular and mitochondrial glutathione redox imbalance in lymphoblastoid cells derived from children with autism. *FASEB J* 2009, 23 (8), 2374–2383. [PubMed: 19307255]
93. Pastore A; Tozzi G; Gaeta LM; Bertini E; Serafini V; Cesare SD; Bonetto V; Casoni F; Carrozzo R; Federici G; Piemonte F, Actin Glutathionylation Increases in Fibroblasts of Patients with

Friedreich's Ataxia: A POTENTIAL ROLE IN THE PATHOGENESIS OF THE DISEASE*. J. Biol. Chem 2003, 278 (43), 42588–42595. [PubMed: 12915401]

94. Nur E; Verwijns M; de Waart DR; Schnog J-JB; Otten H-M; Brandjes DP; Biemond BJ; Elferink RPJO, Increased efflux of oxidized glutathione (GSSG) causes glutathione depletion and potentially diminishes antioxidant defense in sickle erythrocytes. Biochim. Biophys. Acta Mol. Basis Dis 2011, 1812 (11), 1412–1417.

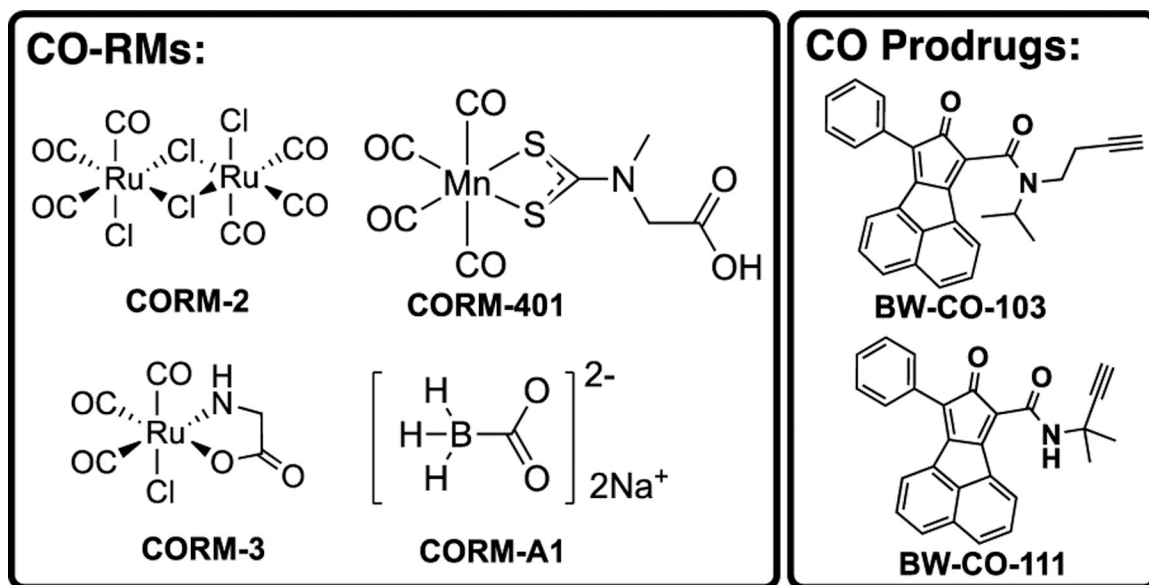


Figure 1.
Structures of representative CO donors.

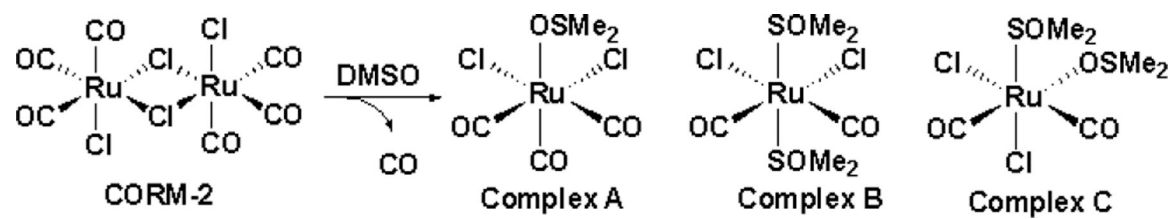


Figure 2.
Speciation of CORM-2 in DMSO.

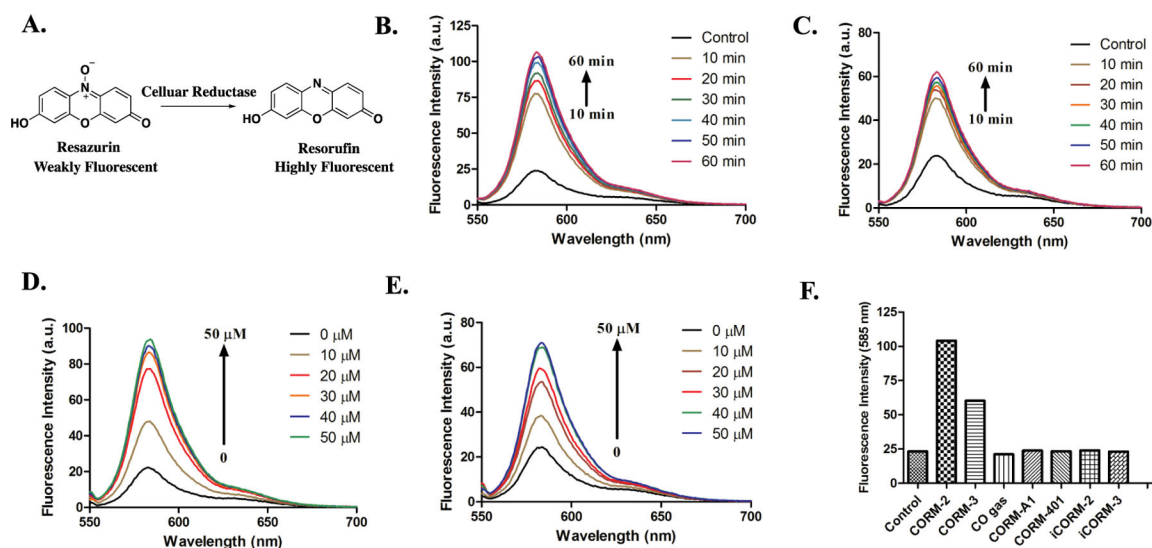
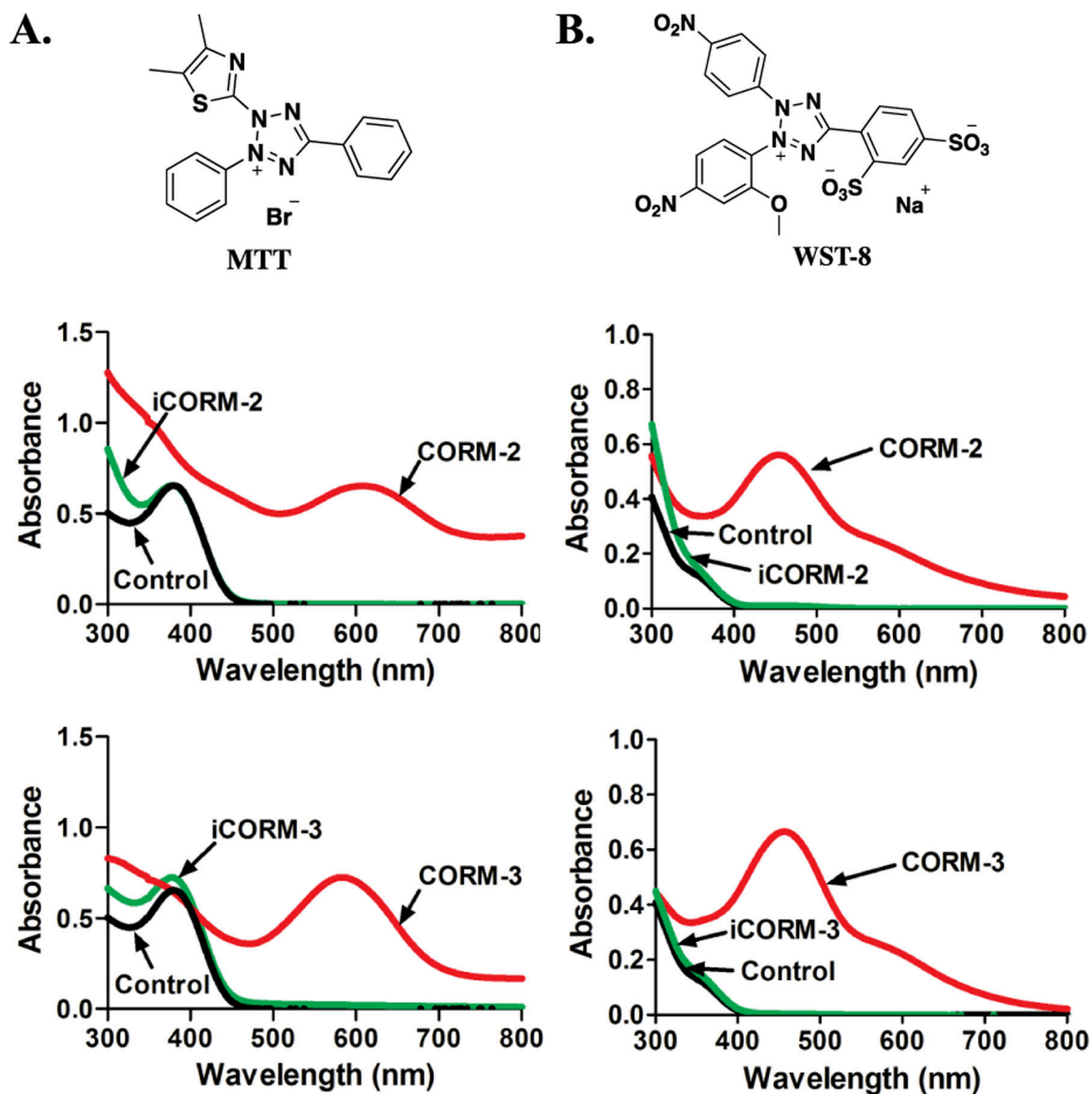


Figure 3.

Responses of resazurin to treatment with various CO donors in PBS (0.01 M, pH = 7.4). A. Mechanism of resazurin-based bioassay. B. The turn-on fluorescence response of 5 μ M resazurin to 50 μ M CORM-2 in PBS at 37 $^{\circ}$ C (λ_{ex} = 550 nm). C. The turn-on fluorescence response of 5 μ M resazurin to 50 μ M CORM-3 in PBS at 37 $^{\circ}$ C (λ_{ex} = 550 nm). D. Fluorescence response of 5 μ M resazurin to various concentrations of CORM-2 after 1 h of incubation in PBS at 37 $^{\circ}$ C (λ_{ex} = 550 nm). E. Fluorescence response of 5 μ M resazurin to various concentrations of CORM-3 after 1 h of incubation in PBS at 37 $^{\circ}$ C (λ_{ex} = 550 nm). F. Fluorescence responses of 5 μ M resazurin to 50 μ M of various CO donors after 1 h incubation in PBS at 37 $^{\circ}$ C (λ_{ex} = 550 nm).



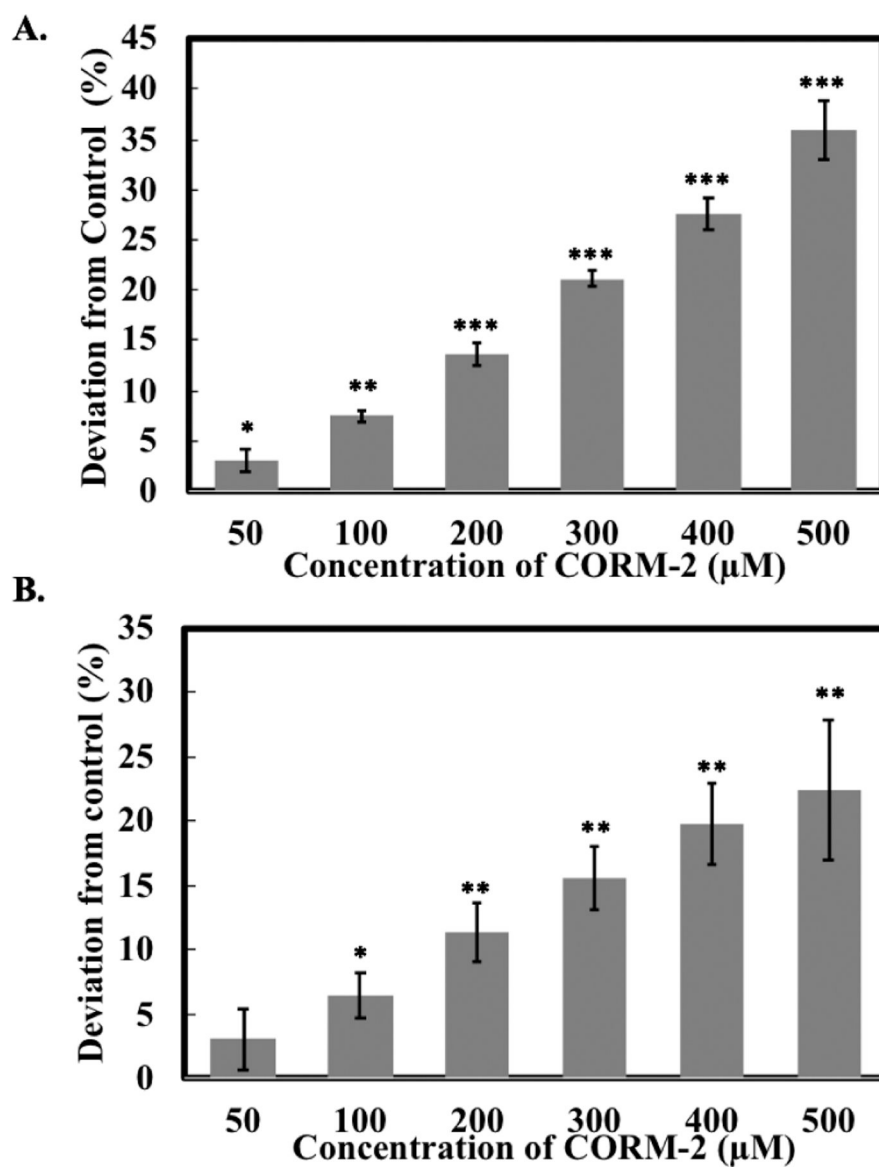


Figure 5. Effects of CORM-2 on A. the CCK-8 assay and B. the resazurin assay. Solutions of CORM-2 in DMEM (10% FBS, 4% DMSO) were incubated for 24 h at 37 °C and then CCK-8 and resazurin assays were performed. The negative control group only contained DMEM (10% FBS). Values are means \pm SD. n = 3. Data with (*), (**) and (***) indicates statistically significant differences between CORM-2 and -3 samples and the negative control as determined by t-test. *P<0.05, **P<0.01, ***P<0.001 versus the control group.

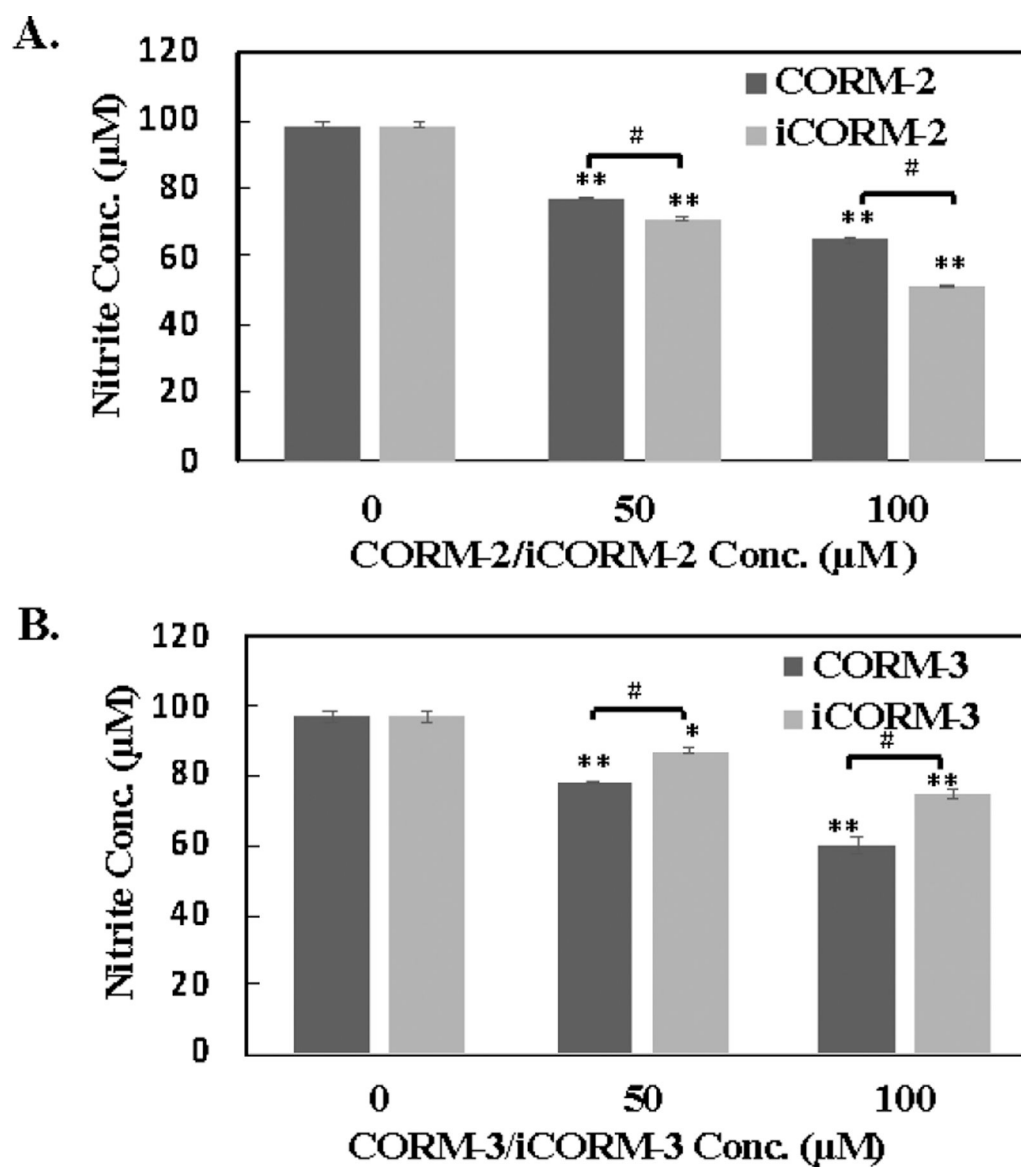


Figure 6. Effects of ruthenium-based CO-RMs on nitrite. A. A solution of 100 μM nitrite in PBS was incubated with CORM-2 and iCORM-2 for 24 h at 37 $^{\circ}\text{C}$ and then nitrite concentrations were determined by the Griess test. B. A solution of 100 μM nitrite in PBS was incubated with CORM-3 and iCORM-3 for 24 h at 37 $^{\circ}\text{C}$ and then nitrite concentrations were determined by the Griess test. Values are means \pm SD. $n = 3$. * $P < 0.01$, ** $P < 0.001$ versus the vehicle group. # $P < 0.001$ between CORMs and iCORMs.

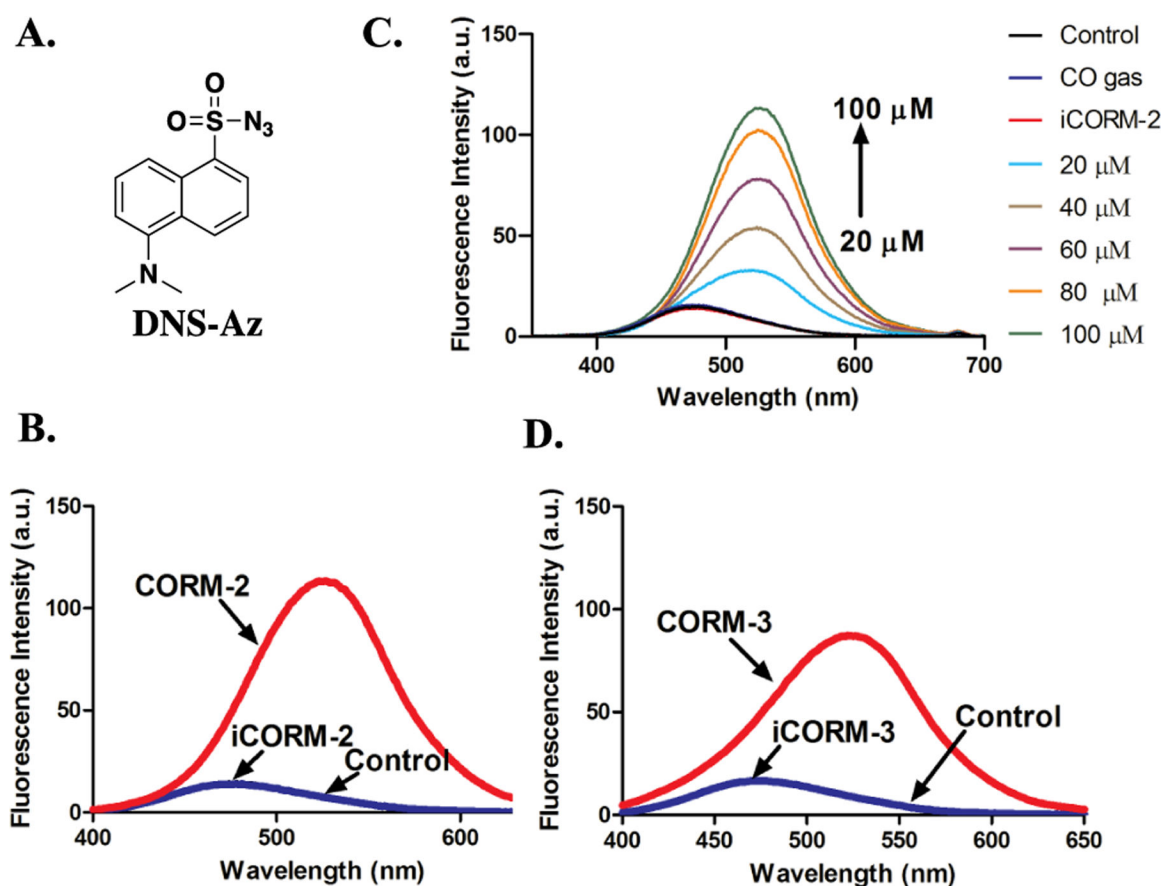


Figure 7. Responses of DNS-Az toward ruthenium-based CO-RMs. A. The structure of DNS-Az. B. Fluorescence response of 100 μM DNS-Az to 100 μM CORM-2 and iCORM-2 in PBS/ACN (1:1) after incubation for 20 min at r.t. ($\lambda_{\text{ex}} = 360$ nm, lines for control and iCORM-2 overlap with each other). C. Fluorescence response of 100 μM DNS-Az to various concentrations of CORM-2, 100 μM iCORM-2 and 10 ml CO gas in PBS/ACN (1:1) after incubation for 20 min at r.t. ($\lambda_{\text{ex}} = 360$ nm, lines for control, CO gas and iCORM-2 overlap with each other). D. Fluorescence response of 100 μM DNS-Az to 100 μM CORM-3 and iCORM-3 in PBS/ACN (1:1) after incubation for 20 min at r.t. ($\lambda_{\text{ex}} = 360$ nm, lines for control and iCORM-3 overlap with each other).

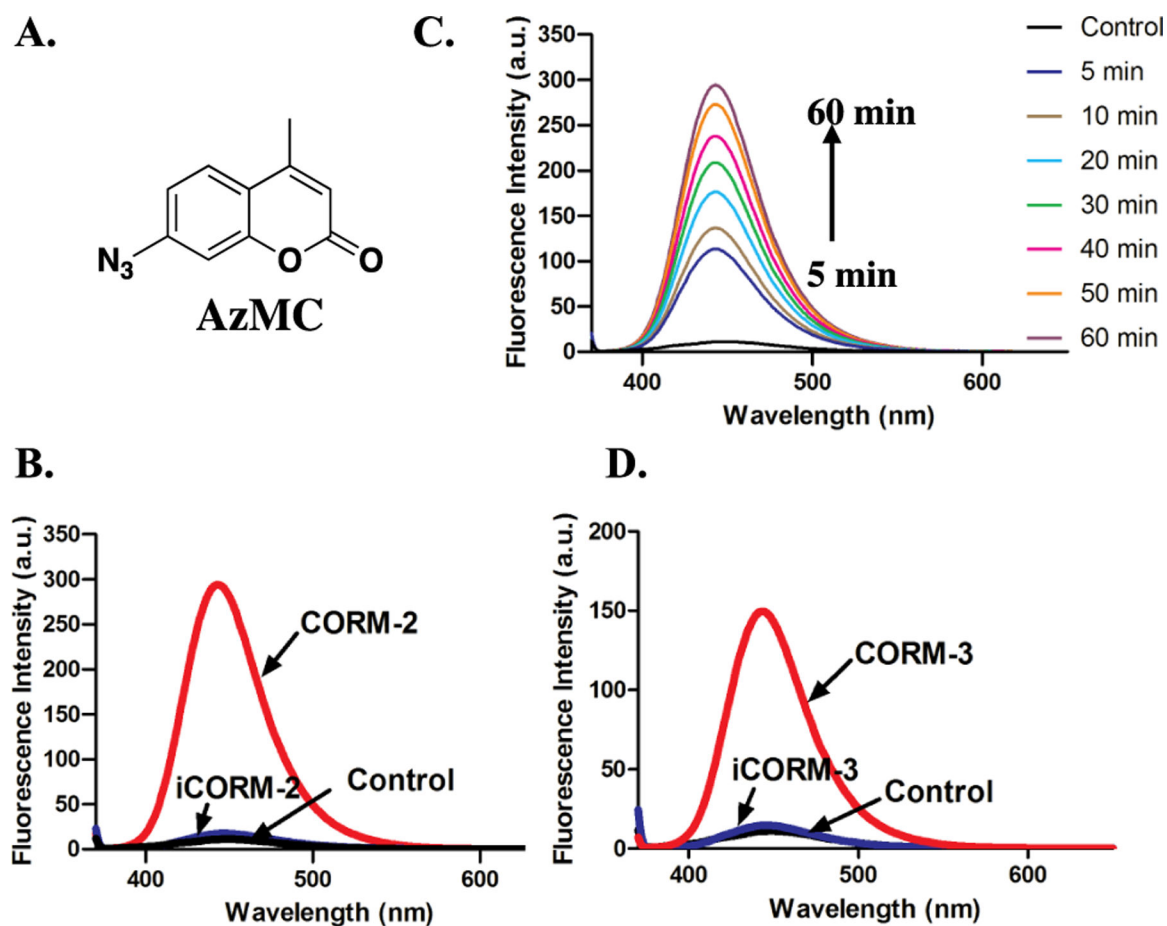


Figure 8.

Responses of AzMC toward ruthenium-based CO-RMs in PBS (0.01 M, pH = 7.4). A. The structure of AzMC. B. Fluorescence response of 10 μ M AzMC to 100 μ M CORM-2 and iCORM-2 in PBS after incubation for 1 h at r.t. (λ_{ex} = 365 nm, lines for control and iCORM-2 overlap with each other). C. Turn-on fluorescence response of 10 μ M AzMC to 100 μ M CORM-2 in PBS at r.t. (λ_{ex} = 365 nm). D. Fluorescence response of 10 μ M AzMC to 100 μ M CORM-3 and iCORM-3 in PBS after incubation for 1 h at r.t. (λ_{ex} = 365 nm, lines for control and iCORM-3 overlap with each other).